Sliding Mode Based DTC of Three-Level Inverter Fed Induction Motor Using Switching Vector Table

Tanvir Ahammad Abdul R. Beig Khalifa Al-Hosani
Department of Electrical Engineering
The Petroleum Institute
Abu-Dhabi, UAE
tahammad@pi.ac.ae bbeig@pi.ac.ae khalhosani@pi.ac.ae

Abstract—**This paper presents two sliding surfaces to control stator flux magnitude and developed torque of the motor. Sliding surfaces enforce the control variables to the respective reference values. A three-level switching vector table (SVT) approach is used to implement sliding mode direct torque control (SM-DTC) of induction motor drive. The SVT is formed using stator flux position in the space vector region of 3L inverter by observing the most significant vector that reflects effective change of flux magnitude and torque in that position. This switching table is simple and gives proper selection of space vector for improved performance of the DTC. Hence, the proposed SM-DTC reduces the complexity of DTC drive, improves the performance of the drive through reducing flux, torque and current ripples. The system is simulated in MATLAB/SIMULINK environment and simulation results are presented to report the improved performance of sliding mode based DTC dive.**

Keywords— Variable Speed Drives; Voltage Source Inverter; DTC; Space Vector PWM.

I. INTRODUCTION

The technological progress in the area of microelectronics, power semiconductor devices and power electronics has opened the opportunities of improving the control strategy of the induction motor drives. Induction motor has been preferred in the industries due to its simple construction, lightweight, ruggedness, inexpensive and minimum maintenance over D.C. motor [1-8]. Several control algorithms of induction motor such as constant v/f control [1-3], field oriented control (FOC) [1-4], direct self control (DSC) [5-6] and direct torque control (DTC) [7-8] have been introduced in the last two decades. The DTC is characterized by simplicity, good performance and robustness. The advantages of three-level (3L) inverter over two-level inverter have attracted specially for modern medium and high power induction motor drives. Therefore several improvements in the form of improving performance, reducing torque and flux ripple has been reported in [9-12] using 3L inverters. In [9-10] multi-level hysteresis band torque controller and flux hysteresis controllers have been used. Most of the DTC techniques for 3L inverted fed induction motor drive reported in literature are based on complex switching table (SVT) [11-12].

The sliding mode control (SMC) is assumed a discontinuous control technique, which has several advantages over traditional controller such as easy to implementation, assures system stability and faster desired response. It also has properties of robustness in external disturbances, order reduction [13-16]. Implementation of SMC implies high-frequency switching. It does not cause any difficulties when electric drives are controlled since the "on-off" operation mode is the only admissible one for power converters [15]. In literature most of the sliding mode based DTC techniques have been proposed incorporating with continuous space vector modulation (SVM) technique instead of classical switching vector method for induction motor DTC [13-18]. The SVM modulation ensures constant switching frequency and smooth current and torque response but it makes the control system complex and computationally demanding for implementation.

In order to reduce the complexity and computational time of DTC a simplified new switching vector table for 3L inverter fed induction motor drives is proposed in this paper. The switching vector table is introduced using the appropriate space vectors which reflect the changes of motor flux and torque in the symmetrical sectors of the space vector regions.

The main objective of this work is to implement a sliding mode based DTC for three-level inverter-fed induction motor using a simple and simplified switching vector table. The dynamic performance of the motor is reported based on the simulation study. The simulation of the proposed control system is carried out for a 4 kW, 400 V, 8.8 A, 50 Hz delta connected three phase squirrel cage induction motor using MATLAB/SIMULINK software.

Section II discusses dynamic modeling of induction motor, section III presents briefly the operation of 3L inverter and space vector diagram of the inverter, section IV explains the basics principle of DTC, section V presents the sliding surfaces of control variables VI details the proposed switching vector table and section VII presents the simulation results of the system.

II. DYNAMIC MODEL OF INDUCTION MOTOR

The dynamic model of induction motor is well published. So, a brief information is given here. The dynamic model in stationary reference frame is given by (1) - (3).

978-1-4673-5769-2/13/$31.00 ©2013 IEEE

$$\underline{v_s} = R_s \underline{i_s} + \frac{d\underline{\psi_s}}{dt} \quad (1)$$

$$0 = R_r \underline{i_r} + \frac{d\underline{\psi_r}}{dt} - j\omega\underline{\psi_r} \quad (2)$$

$$J\frac{d\omega}{dt} = T_m - B\omega - T_{load} \quad (3)$$

The stator flux $\underline{\psi_s}$ and rotor flux $\underline{\psi_r}$ are the function of motor currents such as (4);

$$\underline{\psi_s} = L_s \underline{i_s} + M\underline{i_r} \quad (4a)$$

$$\underline{\psi_r} = L_r \underline{i_r} + M\underline{i_s} \quad (4b)$$

The developed torque of the motor is a function of $\underline{\Psi}_s$ and $\underline{\Psi}_r$ as in (5);

$$T_m = \left(\frac{2}{3}\right)\left(\frac{P}{2}\right)\left(\frac{M}{\sigma L_s L_r}\right)\left(\left|\underline{\psi_s}\right|\left|\underline{\psi_r}\right|\sin\delta\right) \quad (5)$$

Where,

R_s = Stator resistance (Ω) L_s= Stator self-inductance (H)

R_r = Rotor resistance (Ω) L_r = Rotor self-inductance (H)

$\underline{v}_s$ = Stator voltage (V) L_o = Mutual inductance (H)

$\underline{i_s}$ = Stator current (A) J = Motor inertia (Kg-m^2)

$\underline{i_r}$ = Rotor current (A) B=Frictional coeff. (Nm/(rad/sec))

T_m = Motor torque (N-m) T_{load} = Load torque (Nm)

ω = Speed (rad/sec) δ = Angle between Ψ_s & Ψ_r (rad)

III. THREE-LEVEL (3L) INVERTER

The Fig. 1 shows the power circuit of a neutral point diode clamped (NPC) three-level voltage source inverter (VSI). Each phase of this inverter consists of two clamping diodes and four semiconductor switches. The switching states of the inverter are shown in Table I.

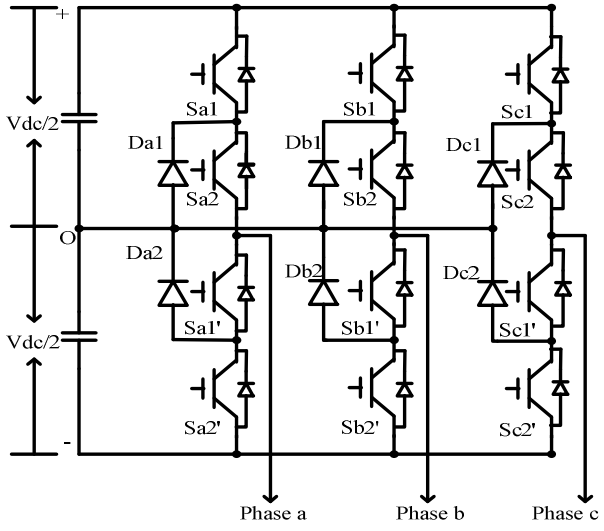

Figure 1: Three-level (3L) inverter circuit

A three phase 3L inverter has 3^3=27 number of switching states, 18 active and three zero vectors. The space vectors associated with the 3L inverter on α-β plan are shown in Fig. 2. The entire space vector region of 3L inverter is divided into six major sectors Z (Z=1, 2, 3, 4, 5 and 6). Each sector is further divided into six symmetrical minor sectors S (S=1, 2, 3, 4, 5 and 6) . This simplifies the 3L space vector analysis [20]. Z and S uniquely define a triangular region by a number given by R = (10*Z+S).

TABLE I: SWITCHING STATUS AND POLE VOLTAGE

Switch Status	Switching State (Sa)	Pole Voltage
Sa1 = ON, Sa2 = ON, Sa1'= OFF, Sa2' = OFF Da1=OFF, Da2 = OFF	+1	$V_{ao} = V_{dc}/2$
*Sa1 = OFF, Sa2 = ON, Sa1'= ON, Sa2' = OFF Da1*and *Da2* will be *ON / OFF* depending on direction of the load current	0	$V_{ao} = 0$
Sa1 = OFF, Sa2 = OFF, Sa1'= ON, Sa2' = ON Da1=OFF, Da2 = OFF	-1	$V_{ao} = -V_{dc}/2$

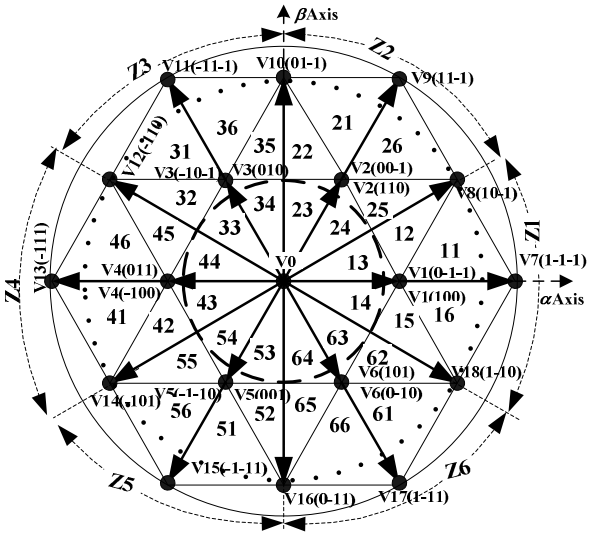

Figure 2: Space vector diagram of 3L inverter

IV. BASIC PRINCIPLE OF DTC

Direct torque control technique uses flux and developed torque of motor as the control variables for controlling the motor drives. In (1), for small $R_s\underline{i}_s$ drop the stator flux is mainly determined by applied voltage vector.

According to (5), developed torque depends on magnitude of stator flux |Ψs|, rotor flux |Ψr| and the angle between stator and rotor flux δ. Ψs can be changed instantly by changing vs. Ψr will change after some time delay. Hence the torque angle δ can be easily changed to increase or decrease the torque according to the voltage vectors of (1).

A complete block diagram of DTC is shown in Fig. 3. It requires two major controllers for controlling magnitude of stator flux & motor torque. A speed controller is used if the target is to control the motor speed. The stator flux, torque and speed of the motor are estimated. A switching vector table is used to select appropriate voltage vector.

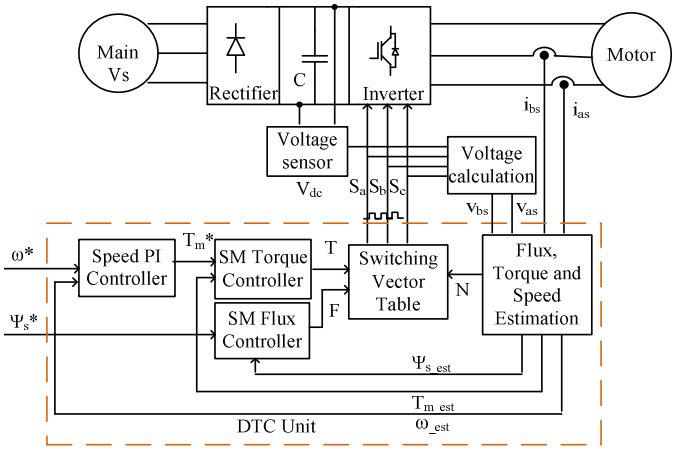

Figure 3: Block diagram of DTC of IM

A. *Estimation of Flux*

The α and β components of stator flux $\underline{\Psi}_s$ can be estimated using the stator voltage as in (6).

$$\psi_{\alpha s} = \int (V_{\alpha s} - i_{\alpha s} R_s)dt \text{ and } \psi_{\beta s} = \int (V_{\beta s} - i_{\beta s} R_s)dt \qquad (6)$$

B. *Estimation of Torque*

The motor torque can be represented as a function of stator flux and currents as follows.

$$T_m = (\frac{2}{3})(\frac{P}{2})(\psi_{\alpha s} i_{\beta s} - \psi_{\beta s} i_{\alpha s}) \qquad (7)$$

The torque estimation requires estimated flux components $\Psi_{\alpha s}$, $\Psi_{\beta s}$ and the current components $i_{\alpha s}$ and $i_{\beta s}$.

C. *Estimation of Speed*

Speed is estimated using (8), has been discussed in [18-19].

$$\omega(t) = \omega_s(t) - \omega_{slip}(t) \qquad (8)$$

Where, $\omega_s(t)$ is the synchronous speed of the motor given by $\omega_s(t) = \frac{d\rho}{dt}$ and $\omega_{slip}(t)$ is the slip speed of the motor are expressed as $\omega_{slip}(t) = \frac{i_{qs}(t)}{T_r i_{mr}(t)}$.

Where, ρ is the unit vector, i_{qs} is stator current on rotor flux frame, i_{mr} is the magnetizing current of the motor.

D. *Speed Controller*

A proportional integral (PI) controller is used to control motor speed. It generates the reference torque for the torque controller.

V. DEGINING OF SLIDING SURFACES

The proposed DTC technique uses sliding mode flux and torque controllers. The main task of the sliding mode (SM) controllers is to achieve fast and reliable torque and flux control. The controller details are discussed below:

A. *Sliding Mode Flux Controller:*

This controller is designed to control the magnitude of stator flux $|\underline{\Psi}_s|$ based on the reference command of the flux magnitude. Therefore sliding surface for the flux controller is designed such that the flux error e_ψ , difference between measured flux $|\underline{\Psi}_s|$ and reference flux $|\underline{\Psi}_s^*|$ becomes zero on sliding surface.

The sliding surface of the flux controller is given by (9).

$$S_\psi = e_\psi + K_\psi \int e_\psi dt \qquad (9)$$

Where, $e_\psi = |\underline{\psi_s}^*| - |\underline{\psi_s}|$ and K_Ψ is a controller design constant.

If the system stays on the surface, then. $S_\psi = 0$. Therefore the time derivative of the sliding surfaces will also be zero, as a result time derivative of (9) yields,

$$\frac{de_\psi}{dt} = K_\psi e_\psi \qquad (10)$$

Which gives an exponential convergence of e_ψ to the sliding surface with a rate of K_Ψ. The block diagram of flux controller is shown in Fig. 4(a).

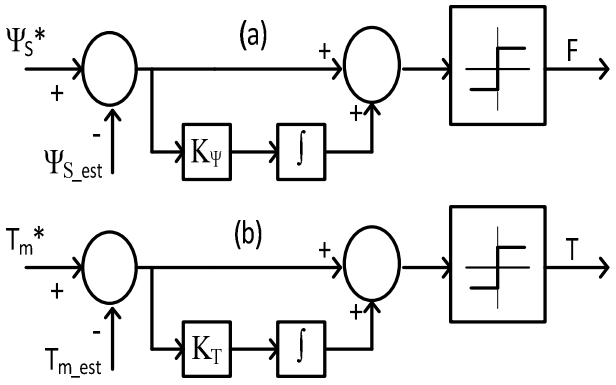

Figure 4: (a) SM flux controller (b) SM torque controller

B. *Sliding Mode Torque Controller:*

Torque controller is also a sliding mode controller. Similar sliding surface as flux controller is designed to control torque of the motor. The torque error e_T is applied to this controller and the sliding surfaces enforces motor torque T_m to the commanded reference torque T_m^*. The sliding surface of the torque controller is in (10).

$$S_T = e_T + K_T \int e_T dt \qquad (11)$$

Where $e = T_m^* - T_m$ and K_T is a controller design constant.

If sliding mode exists then $S_T = 0$ the time derivative of the sliding surface S_T' will also be zero. Therefore time derivative of (11) gives (12).

$$\frac{de_T}{dt} = K_T e_T \qquad (12)$$

The solution of this first order dynamic is an exponential convergence of e_T to the sliding surface with a rate of K_Ψ. The block diagram of torque controller is shown in Fig. 4(b).

VI. Proposed Switching Vector Table

Assuming $R_s\underline{i}_s$ drop is small; change of the stator flux with the space vectors of inverter can be expressed using Euler's rule in (1) such that $\underline{\psi}_s = \underline{\psi}_{sO} + \underline{v}_s t$. Where, $\underline{\Psi}_{s0}$ is the stator flux at t=0.

By selecting the appropriate voltage vectors stator flux $|\underline{\Psi}_s|$ can be kept nearly a constant flux shown in Fig. 5. Similarly torque angle δ also can be increased or decreased with that vector selection which controls the torque of the motor by (5).

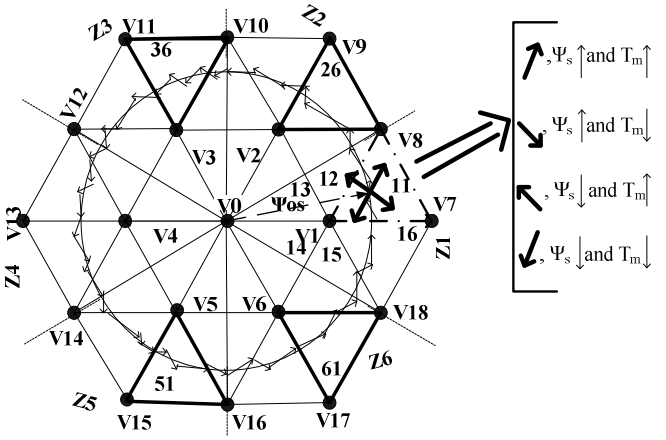

Figure 5: Change of flux and torque with the space vector

To select the proper voltage vector, exact position of the flux is required. Depending on that position voltage vectors are selected to satisfy the flux and torque demand. For each R, the switching vector table is derived by observing the most significant vectors.

TABLE III: SWITCHING VECTOR TABLE

	R=10Z+S; S=1, 2	***R=10Z+S; S = 3, 4***	***R=10Z+S; S= 5, 6***
F=1 ***T=1***	Large vector of triangle **U**	Small vector of triangle **U**	Medium vector of triangle **U**
F=1 ***T=-1***	Medium vector of triangle **V**	Small vector of triangle **V**	Large vector of triangle **V**
F=-1 ***T= 1***	Large vector of triangle **W**	Small vector of triangle **W**	Medium vector of triangle **W**
F=-1 ***T=-1***	Medium vector of triangle **X**	Small vector of triangle **X**	Large vector of triangle **X**

Where,

U *= rem((10*(Z+1)+6),70);* *If (**U** > 0 && **U** < 20)* ***U****=**U**+10;*	***V*** *= rem((10*(Z+5)+1), 70);* *If (**V** > 0 && **V** < 60)* ***V****=**V**+10;*
W *=rem((10*(Z+2)+6), 70);* *If (**W** > 0 && **W** < 30)* ***W****=**W**+10;*	***X*** *= rem((10*(Z+4)+1), 70);* *If (**X** > 0 && **X** < 50)* ***X****=**X**+10;*

From Fig. 5 it is observed that for R=11, 12, 15, and 16 the most effective vectors are associated with the end points of highlighted triangles. Similarly for every R, triangles are chosen to identify exact vector that gives the most effective change of flux and torque given in Table II. This vector selection gives single switching and minimum change in line voltage from one vector to another vector throughout a cycle.

VII. Simulation Results

A squirrel cage induction motor rated of 5 hp, 400 V, 8.8 A, 50 Hz with delta connected windings is considered to implement proposed SM-DTC technique. The open circuit and block rotor test has been done to calculate the parameters of the motor. The parameters are given in Appendix.

Flux, torque and speed are estimated using the model equations discussed in respective sections. A first order low pass filter is used in the speed estimation block to eliminate ripple in the estimated speed. The cut off frequency of the filter is 1 kHz.

The controller design constants K_Ψ, K_T and PI controller constants K_P and K_I are also given in Appendix.

The sampling time of the simulation is 20 µs. A step change full load torque is applied at stable state of motor at 4 s. The reference speed is set up at 1400 rpm and reference flux is set up at rated flux 1.56 wb.

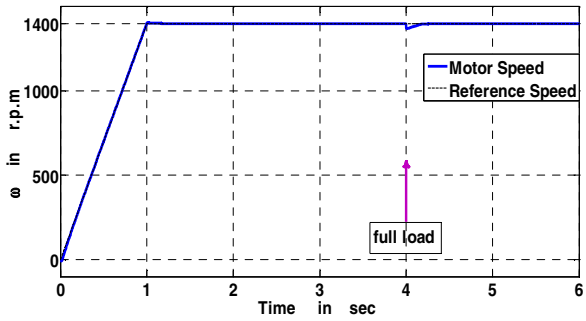

Figure 6: Speed response with full load at 4s

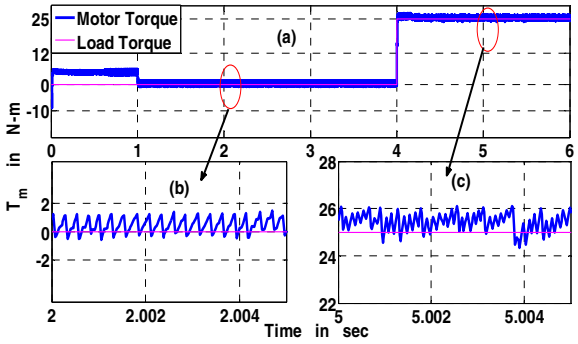

Figure 7: (a) Torque response (b) expanded in scale at steady-state at no load (c) expanded in scale at steady state at full load

Figure 6 presents speed response of the motor. The motor speed tracks the reference speed command. The percentage overshoot is 0.3 % calculated. The torque response of the drive is shown in Fig. 7. For a step change of full load torque motor drive torque response of 7 ms is achieved. From Fig. 7(b)

torque response under no load condition at steady-state is observed. The torque response in time expanded scale under full load condition at steady-state is shown in Fig. 7(c). The percentage of torque ripple at full load is 1.3% and at no load this is 6.7%. The ripple switching frequency is limited to 12k Hz.

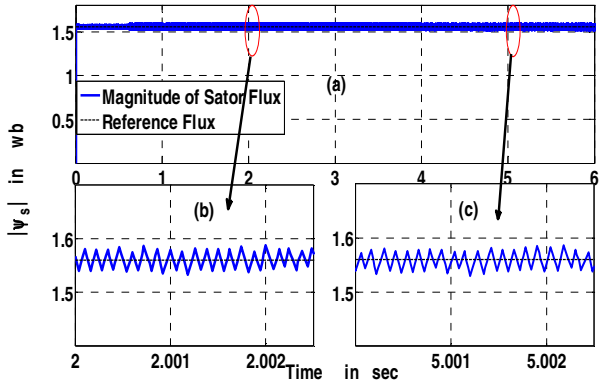

Figure 8: (a) Flux response with a load (b) expanded in scale at steady-state at no load (c) expanded in scale at steady-state at full load

Fig. 8 shows the flux response of the motor. The time scale expanded stator flux both at no load and full load condition are presented in Fig. 8(b) and 8(c). The percentage of the flux ripple is 1.92 % determined.

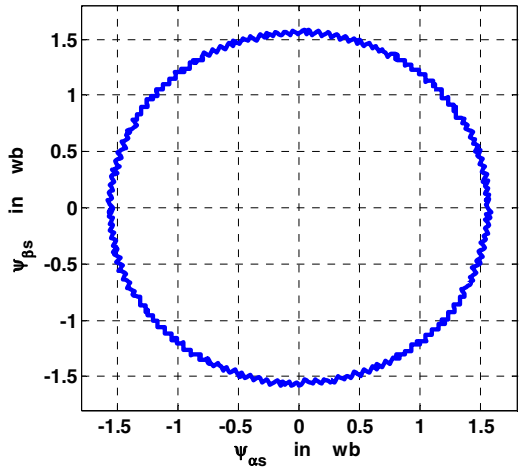

Figure 9: Trajectory of stator flux

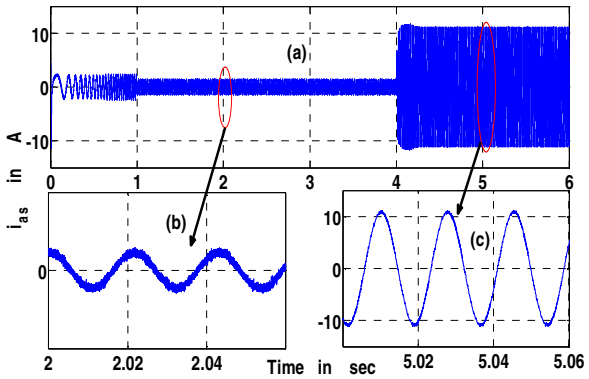

Figure 10: (a) Stator line current response (b) expanded in scale at steady state at no load (c) expanded in scale at steady-state at full load.

The trajectory of the stator flux is presented in Fig. 9, it shows the magnitude of the flux remains constant throughout a complete cycle and magnitude is rated flux 1.56 wb as so reference flux.

The behavior of current response is presented in Fig. 10. The transient response is displayed by Fig. 10(a). At the starting of the motor there is a current of 11.18 A which is within the range of motor rated peak current.

The stator line voltage is given by Fig. 11. The frequency of the line voltage is 55.9 Hz. The fast fourier transform analysis of the line voltage and current are shown in Fig. 12 and Fig. 13. In Fig. 12 it can be seen that the harmonics are dominant near switching frequency. The Fig. 13 shows that the harmonic currents are very small.

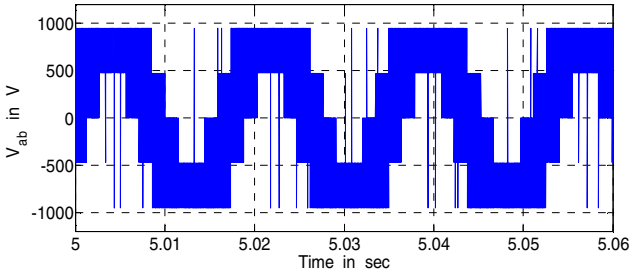

Figure 11: Stator line voltage at steady-state

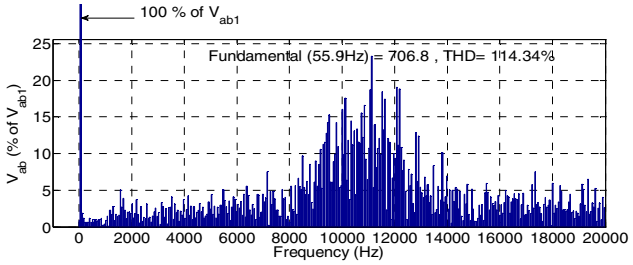

Figure 12: Harmonic spectrum of v_{ab}

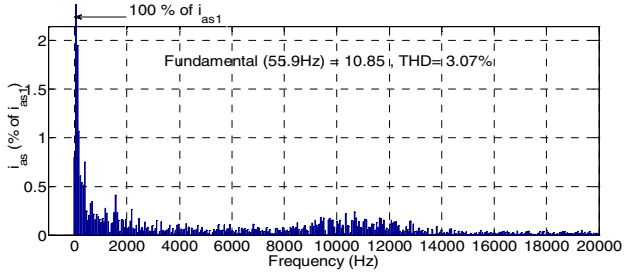

Figure 13: Harmonic spectrum of i_{as}

A sudden reversal speed command is also set up for investigating the dynamic performance of the drive. The speed from +1400 rpm to -1400 is commanded at 1s. Figure 14 presents the speed response of the motor with the reverse speed command and it shows motor reacts on change the direction of reference speed. A full load torque is applied at 4 s. The current response of the motor with reversal speed is given in Fig. 15. At zero crossing speed the peak value of the line current is 2.19 A. At steady-state motor draws full load

current at full load condition. The peak value of the current is 10.6 A.

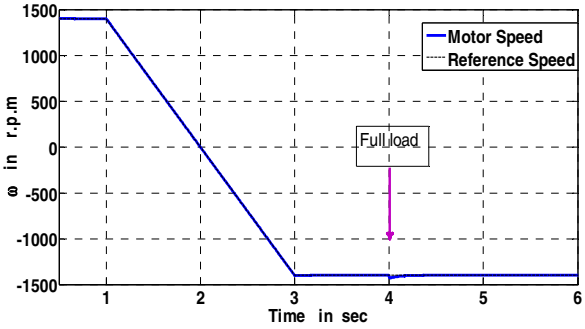

Figure 14: Speed response at reversal speed command

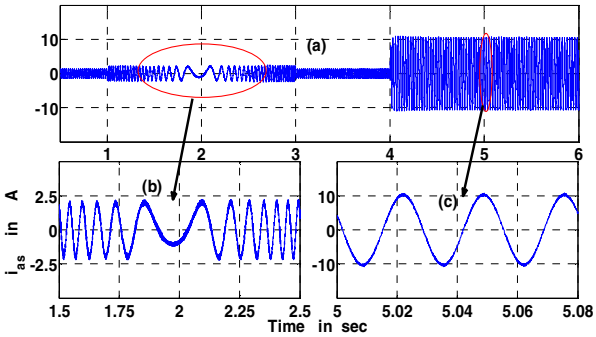

Figure 15: (a) Stator line current for a reversal speed command (a) expanded in scale at zero crossing speed (b) expanded scale at steady-state at full load

VIII. CONCLUSION

A sliding mode based direct torque control of IM drive is presented using three-level inverter space vectors. A simple and accurate switching vector table is formed to establish the control technique for improving dynamic performance of the drive. Simulation results are presented. The fast and improved flux and torque responses are pointed out. The simplicity and performance of the drive say proposed SM-based DTC is suitable for three-level inverter fed induction motor drives.

APPENDIX

Simulation Parameters: R_s = 4.6023 Ω; R_r = 4.94 Ω; L_s = 0.7973 H; L_r = 0.7973 H; M = 0.768 H; J = 0.03 Kg-m^2; B = 3.17e3 N-m/(rad/sec); P = 4; N = 1432 rpm.

$K_\Psi = K_T$ = 0.01, K_P = 0.8 N-m/(rad/sec) and K_I = 7 N-m/(rad/sec^2). The D.C. link voltage, V_{dc} = 950 V.

REFERENCES

[1] Vas, Peter, 'Vector Control of A.C. Machines', Oxford University Press, New York, 1990.

[2] Muhammad H. Rashid, 'Power Electronics circuits, devices, and applications ', Pearson prentice Hall 2004.

[3] James N. Nash, "Direct Torque Control, Induction Motor Vector Control without an Encoder", *IEEE Transactions on Industry Applications,* Vol. 33, no. 2, March/April 1997.

[4] Alfio Consoli, Giuseppe Scarcella, and Antionio Testa, "Slip-Frequency Detection for Indirect Field-Oriented Control Drives", *IEEE Transaction on Industry Applications,* vol. 40, no. 1, January/February 2004.

[5] M. Depenbrock, "Direct Self-Control (DSC) of Inverter-Fed Induction Machine", *IEEE Transactions on Power Electronics,* vol. 3, no. 4, Oct. 1988.

[6] U. Baader, M. Depenbrock, and G. Gierse, "Direct self-control (DSC) of inverter-fed-induction machine - A basis for speed control without speed measurement", *IEEE Trans. Ind. Applicat.*, Vol. 28, pp. 581-588, May/June 1992.

[7] Takahashi, T. Noguchi, "A New Quick-Response and High-Efficiency Control Strategy of Induction Motor", *IEEE Transaction on Industrial Applications,* vol. 22, no. 5, Sept/Oct. 1986.

[8] Isao Takahashi and, Youichi Ohmori, "High-Performance Direct Torque Control of an Induction Motor", *IEEE Transactions on Industry Applications*, vol. 25, No. 2, March 1989.

[9] Maurizio Cirrincione, Marcello Pucci, and Gianpaolo Vitale, "Direct Torque Control for Three-Level Fed Induction Motor Drives with Capacitor Voltage Ripple Minimization*", IECON, 2008: The 34th Annual Conference of the IEEE Industrial Electronics Society,* Nov 2008.

[10] Kyo-Beum Lee, Joong-Ho Song, Ick Choy, and Ji-Yoon Yoo, "Torque Ripple Reduction in DTC of Induction Motor Driven by Three-Level Inverter With Low Switching Frequency", *IEEE Transactions on Power Electronics,* vol. 17, No. 2, March 2002.

[11] Xavier del Toro Garcia, Antoni Arias, Marcel G. Jayne, Phil A. Witting, Vicenc M. Sala, and Jose Luis Romeral, "New DTC control Scheme for Induction Motors fed with a Three-level Inverter", *Proceedings of the IEEE International Symposium on Industrial Electronics, ISIE 2005,* volume 4, June 2005.

[12] Yongchang Zhang, Zhengming Zhao, Janguo, Wei Xu, and D. G. Dorrell, "Speed Sensorless Direct Torque Control of 3-Level Inverter-Fed Induction Motor Drive Based on Optimized Switching Table", *IECON, 2009: The 35th Annual Conference of the IEEE Industrial Electronics Society,* Nov 2009, pages: 1316-1321.

[13] C. Lascu, Ion Boldea, and F. Blaabjerg, "Direct Torque Control of Sensorless Induction Motor Drives: A Sliding-Mode Approach", *IEEE Transactions on Industry Applications,* vol. 40, no. 2, March/April 2004.

[14] Shir-Kuan Lin, and Chih-Hsing Fang, "Sliding-Mode Direct Torque Control of an Induction Motor", *IECON'01: The 27th Annual Conference of the IEEE Industrial Electronics Society.*

[15] Vadim I. Utkin, "Sliding Mode Control Design Principles and Applications to Electric Drives", *IEEE Transactions on Industrial Electronics,* vol. 40, no. 1, February 1993.

[16] Vadim Utkin, Jurgen Guldner, and Jingxin Shi, Sliding Mode Control in Electromechanical Systems, CRC Press, 1999.

[17] S. Ryvkin, R. Schmidt-Obermoeller, and A. Steimel, "Sliding-Mode-Based Control for a Three-Level Inverter Drive", *IEEE Transaction on Industrial Electronics,* Vol. 55, no. 11, November 2008.

[18] Abdul R. Beig, and V. T. Ranganathan, "A novel CSI-Fed Induction Motor Drive", *IEEE Transactions on Power Electronics,* vol. 21, no. 4, July 2006.

[19] Ahmed Shehada, Abdul R. Beig, "An Improved CSI fed Induction Motor Drive", *International Journal of Electrical Power and Energy Systems,* vol.46, pg. 26-35, 2013.

[20] Abdul R. Beig, and V. T. Ranganathan, "Influence of Placement of Small Vectors on the Performance of PWM Techniques for Three-Level Inverters", *IECON, 2003: The 29th Annual Conference of the IEEE Industrial Electronics Society,* Nov 2003, 2764 - 2770 Vol.3.